Highly luminescent $Gd_2O_2S:Er^{3+},Yb^{3+}$ upconversion microcrystals obtained by a time- and energy-saving microwave-assisted solid-state synthesis

Ian P. Machado [a,b,c,*], Jur de Wit [b], Arnoldus J. van Bunningen [b], Cássio C.S. Pedroso [d], Lucas C.V. Rodrigues [c], Hermi F. Brito [c], Andries Meijerink [b]

[a] Department of Chemistry, University of Turku, FI-20014 Turku, Finland
[b] Condensed Matter and Interfaces, Debye Institute for Nanomaterials Science, Utrecht University, 3584CC Utrecht, The Netherlands
[c] Department of Fundamental Chemistry, Institute of Chemistry, University of São Paulo, 05508-000, Brazil
[d] The Molecular Foundry, Lawrence Berkeley National Laboratory, Berkeley, CA 94720, USA

ARTICLE INFO

ABSTRACT

Er^{3+}-doped and Er^{3+},Yb^{3+}-co-doped Gd_2O_2S are one of the most efficient upconversion (UC) materials available to date. However, preparing lanthanide oxysulfides can be challenging as it requires several hours of heating at > 1000 °C in high power furnaces. Nonetheless, in designing a new synthesis technology for UC materials, one should consider that these systems suffer from defect quenching, responsible for significant optical energy losses. In this work, the microwave-assisted solid-state (MASS) synthesis was explored as an alternative to synthesize this class of materials, using two different starting compounds – lanthanide oxides (Ln_2O_3) and hydroxycarbonates ($Ln(OH)CO_3$), where Ln^{3+}: Gd, Er, Yb. Different Er^{3+},Yb^{3+} concentrations were investigated, and the $Er^{3+}_{(5\%)},Yb^{3+}_{(5\%)}$ and $Er^{3+}_{(1\%)},Yb^{3+}_{(10\%)}$ were shown to give the most intense UC output comparable to commercially available materials. Using $Ln(OH)CO_3$ instead of the more common Ln_2O_3 for the MASS synthesis contributed to higher UC efficiencies and a more homogeneous Er^{3+} and especially Yb^{3+} distribution through the Gd_2O_2S lattice as verified by luminescence lifetime measurements. These high-quality materials were prepared in a simple two-step synthesis of 50 min and using a domestic microwave oven, leading to a remarkable decrease of 79% in processing time and 93% in energy consumption, making the MASS method suitable to be explored as an alternative synthesis methodology for high performance UC materials.

1. Introduction

Upconversion (UC) is a non-linear optical phenomenon in which a material absorbs two or more low energy photons, *e.g.* near-infrared (NIR) photons, to combine their energy into a single high energy photon, *e.g.* visible light. This phenomenon was first experimentally observed by Auzel for the Er^{3+}/Yb^{3+} pair in 1966, and henceforth it became an active area of research in lanthanide (Ln) spectroscopy [1,2]. The well-defined ladder-like structure of several Ln^{3+} energy level schemes is suitable for UC processes, especially for the Er^{3+} ion and the Er^{3+},Yb^{3+} ion pair producing highly efficient UC materials [3,4]. Currently, research on Er^{3+}-doped and Er^{3+},Yb^{3+}-co-doped UC materials touches diverse sectors in technology. For example, bulk $NaYF_4:Er^{3+}$ and $Gd_2O_2S:Er^{3+}(,Yb^{3+})$ systems were investigated as solar cell sensitizers to upconvert the infrared portion of the solar spectrum [5–7], which is not absorbed by conventional c-Si solar cells, while $NaYF_4:Er^{3+},Yb^{3+}$ nanoparticles have been explored as devices for bioimaging of cells and small animals, as well as for photodynamic therapy [2,8,9]. In many banknotes (*e.g.* Euro and Renminbi) Yb/Er-doped upconversion materials are incorporated as anti-counterfeiting feature.

Regardless of the technological target, there is a need for optimizing the quantum efficiency, which is around 10% for the best UC materials [10]. One of the most suitable host matrices to yield high quantum UC is gadolinium oxysulfide – Gd_2O_2S, due to its high chemical/thermal stability and low phonon energy ($\sim$440 cm^{-1}) [11,12], which reduces quenching of the excited energy levels *via*

---

lattice vibration. Preparing Gd_2O_2S-based UC materials, however, is a tricky task. Conventional solid-state synthesis methods based on resistive heating are normally used [13–15], which employs high temperatures (> 1000 °C) for times exceeding 4 h in ovens and consume over 10 kWh. In addition, several heating-cooling steps may be needed, together with inert/reducing atmospheres, to prevent contaminant phases such as Gd_2O_3. These steps are necessary to improve purity of the final product, but they also drastically increase synthesis time and energy consumption, thus rising production costs. From a time, cost and environmental perspective, an energy-saving synthesis procedure for Gd_2O_2S is highly interesting. However, it is crucial that with such method, high-quality UC materials are obtained on both laboratory and industrial scale without sacrificing their optical properties.

It is worth emphasizing that the crystal purity of a material strongly influences its UC efficiency as impurities and point defects in the structure can act as quenching pathways that reduce the materials' UC emission [16]. UC materials rely on energy migration and transfer and are therefore more prone to concentration quenching by defects/impurities than simple one-to-one photon conversion materials. In this context, this work explores the rapid microwave-assisted solid-state (MASS) synthesis as an alternative methodology to synthesize Gd_2O_2S-based UC materials. A series of single-doped Gd_2O_2S:Er^{3+} and co-doped Gd_2O_2S:Er^{3+},Yb^{3+} materials were prepared in a fast two-step synthesis, totaling 50 min of microwave radiation exposure to the precursors. Two distinct precursors, Ln_2O_3 and $Ln(OH)CO_3$ (Ln^{3+}: Gd, Er, and Yb) were used in order to optimize the materials' crystallinity and UC performance. When excited by a 980 nm diode laser, the materials synthesized by the MASS method exhibited UC emission intensities comparable to those from commercial samples with the same nominal Er^{3+} and Yb^{3+} concentrations. The highest UC emission intensity was achieved for the Gd_2O_2S:$Er^{3+}_{(1\%)}$,$Yb^{3+}_{(10\%)}$ material prepared using $Ln(OH)CO_3$ as precursors, which nearly matches the UC intensity of its commercial counterpart. This work demonstrates the MASS method as an effective alternative to prepare highly luminescent Gd_2O_2S:Er^{3+} and Gd_2O_2S:Er^{3+},Yb^{3+} bulk materials, which could be scaled up to supply UC materials for emerging applications.

2. Experimental section

2.1. Chemicals and reagents

Lanthanide oxides (Gd_2O_3 99.99%, Er_2O_3 99.99%, and Yb_2O_3 99.99%, Smart Elements), elemental sulfur (S 99.5%, Alfa Aesar), sodium carbonate, anhydrous (Na_2CO_3 ≥99.5%, Alfa Aesar), nitric acid (HNO_3 ≥65%, Merck), urea ((NH_2)$_2CO$ analytical grade, Merck), acetone ((CH_3)$_2CO$ analytical grade, Merck), and activated carbon (analytical grade, Alfa Aesar) were used as received.

2.2. Synthesizing upconversion (UC) materials by the MASS method

The microwave-assisted solid-state (MASS) method was previously investigated by some of us in the preparation of Ln_2O_2S-based scintillators and persistent luminescence materials [17–19]. In this work, a series of single-doped Gd_2O_2S:Er^{3+} and co-doped Gd_2O_2S:Er^{3+},Yb^{3+} UC materials was synthesized by the MASS method, with varying Er^{3+} dopant and Yb^{3+} co-dopant concentrations, as well as the Ln source to the synthesis. In preparing material precursors, Ln_2O_3 (total lanthanide content, where Ln^{3+}: Gd, Er, and Yb), S, and Na_2CO_3 were weighted in a Ln_2O_3:S:Na_2CO_3 molar ratio of 1:1.1:0.25. The powder mixture was ground with acetone to aid homogenizing and then left to dry in air.

Additionally to Ln_2O_3, lanthanide hydroxycarbonates – Ln (OH)CO$_3$ were also investigated as the Ln^{3+} source for the MASS synthesis. These compounds were synthesized following a literature procedure [20,21], identical for Gd, Er, and Yb. Approximately 10 g of Ln_2O_3 was dissolved into 8–10 mL of boiling concentrated HNO_3. After 30 min of stirring, the pH was registered to be 6–7. The solution was filtered to eliminate the small amount of undissolved Ln_2O_3 powder, and the resultant $Ln(NO_3)_3$ solution was transferred to a 250 mL round flask. Then, 35.0 g of urea previously dissolved in 100 mL of warm (~60 °C) deionized water, was added to this flask, which was heated up to boiling under stirring. Instantaneous precipitation was observed once boiling started, indicating the formation of the desired $Ln(OH)CO_3$. The suspension was left boiling for 270 min after the beginning of precipitation and then left to cool down to room temperature. Finally, the precipitate was washed with deionized water to eliminate NH_4^+ and NO_3^- ions, and the obtained $Ln(OH)CO_3$ powder was dried at 100 °C for 60 min.

After drying, 0.5 g of the prepared precursor mixture was added to a 2.5 cm^3 alumina crucible, formerly surrounded by 11 g of granular activated carbon, and placed inside a bigger 27 cm^3 alumina crucible (Figure S1a, Supporting Information). This bigger crucible, now containing the smaller one which holds the precursor mixture, was covered with an alumina lid and then placed inside the cavity of aluminosilicate thermal insulation bricks. The precursors were heated in a domestic microwave oven (Daewoo KOR1N4A, 1 kWh) using a microwave program of 25 min (Figure S1b), in which the first 10 min the power was set to 90%, and to 80% for the final 15 min. Finally, the obtained material was ground with acetone and adding sulfur powder (10% in mass) to be reheated in the microwave oven using the same power/time program. After the second microwave heating treatment, the resultant Gd_2O_2S:Er^{3+} or Gd_2O_2S:Er^{3+},Yb^{3+} powder was ground (without acetone) to obtain the final materials.

In this context, 8 different Gd_2O_2S-based UC materials were synthesized by using Ln_2O_3 as precursors – 2 single-doped Gd_2O_2S:Er^{3+} and 6 co-doped Gd_2O_2S:Er^{3+},Yb^{3+} materials, with distinct Er^{3+} and Er^{3+},Yb^{3+} concentrations which are displayed in Table 1. Additionally, 8 more materials – with the same Er^{3+} and Er^{3+},Yb^{3+} concentrations – were synthesized using Ln(OH)CO$_3$ as the Ln source. Therefore, 16 materials UC materials were prepared by the MASS method in this work (Table 1). The Er^{3+} and Er^{3+},Yb^{3+} concentration values were selected to match the nominal concentrations of commercial samples of Gd_2O_2S:Er^{3+} and Gd_2O_2S:Er^{3+},Yb^{3+} that were custom made by Leuchtstoffwerk Breitungen GmbH – Germany and Tailorlux GmbH – Germany, to allow for a direct comparison of UC emission intensities between the commercially available materials and the materials prepared by the MASS methodology.

2.3. Characterization and spectroscopic methods

X-ray diffraction (XRD) patterns for Gd_2O_2S:Er^{3+} and Gd_2O_2S:Er^{3+},Yb^{3+} UC materials prepared by the MASS method were registered using a Philips PW1700 diffractometer, with CuKα

Table 1

Overview of Gd_2O_2S-based upconversion (UC) materials synthesized by the microwave-assisted solid-state (MASS) method, displaying the Er^{3+} and Yb^{3+} concentrations as well as the Ln^{3+} source compound used in the syntheses: lanthanide oxides – Ln_2O_3, or lanthanide hydroxycarbonates – $Ln(OH)CO_3$, where Ln^{3+}: Gd, Er, and Yb.

Yb^{3+} (mol-%)	Er^{3+} (mol-%)	Ln^{3+} source compound		
		Ln_2O_3	$Ln(OH)CO_3$	
0	5.0	Gd_2O_2S: $Er^{3+}_{(5\%)}$	Gd_2O_2S: $Er^{3+}_{(5\%)}$	
	10.0	$Er^{3+}_{(10\%)}$	$Er^{3+}_{(10\%)}$	
5.0	1.0	$Er^{3+}_{(1\%)}$, $Yb^{3+}_{(5\%)}$	$Er^{3+}_{(1\%)}$, $Yb^{3+}_{(5\%)}$	
	5.0	$Er^{3+}_{(5\%)}$, $Yb^{3+}_{(5\%)}$	$Er^{3+}_{(5\%)}$, $Yb^{3+}_{(5\%)}$	
	10.0	$Er^{3+}_{(10\%)}$, $Yb^{3+}_{(5\%)}$	$Er^{3+}_{(10\%)}$, $Yb^{3+}_{(5\%)}$	
10.0	1.0	$Er^{3+}_{(1\%)}$, $Yb^{3+}_{(10\%)}$	$Er^{3+}_{(1\%)}$, $Yb^{3+}_{(10\%)}$	
	5.0	$Er^{3+}_{(5\%)}$, $Yb^{3+}_{(10\%)}$	$Er^{3+}_{(5\%)}$, $Yb^{3+}_{(10\%)}$	
	10.0	$Er^{3+}_{(10\%)}$, $Yb^{3+}_{(10\%)}$	$Er^{3+}_{(10\%)}$, $Yb^{3+}_{(10\%)}$	

radiation (1.5418 Å), measuring in the 10–70° 2θ range and employing a 0.02° step with 1 s integration time.

Scanning electron microscopy (SEM) images of the $Gd_2O_2S:Er^{3+}_{(10\%)}$ and $Gd_2O_2S:Er^{3+}_{(1\%)},Yb^{3+}_{(10\%)}$ materials, prepared using both Ln_2O_3 and $Ln(OH)CO_3$ as precursors, were registered using a Phenom ProX Desktop Scanning Electron Microscope, operating at 10 keV. Samples were prepared by depositing a thin layer of UC powder onto a conducting carbon tape.

UC emission spectra of $Gd_2O_2S:Er^{3+}$ and $Gd_2O_2S:Er^{3+},Yb^{3+}$ UC materials prepared by the MASS method, as well as commercial samples, were measured with an Edinburgh Instruments FLS-920 spectrofluorometer, equipped with a 500 mW continuous wave (CW) 980 nm diode laser as the excitation source and a Hamamatsu R928 photomultiplier tube (PMT) as the detector. As the laser spot size was 3x3mm^2 and a 5% neutral density filter was used, the average laser power density was calculated to be approximately 0.3 W/cm^2. Emission was collected at a 90° angle, with the sample holder tilted at 45°. It is worth noting that, to record the UC emission spectra of the $Gd_2O_2S:Er^{3+}$ and $Gd_2O_2S:Er^{3+},Yb^{3+}$ materials, all optical components involved were fixed, as well as the sample volume contained by the sample holder, so that the detected UC intensities could be directly compared. In this way, the UC emission spectra of commercial $Gd_2O_2S:Er^{3+}$ and $Gd_2O_2S:Er^{3+},Yb^{3+}$ samples from Leuchtstoffwerk Breitungen and Tailorlux could be compared with those of the materials obtained by MASS method.

Lifetime measurements were also performed on the $Gd_2O_2S:Er^{3+}_{(10\%)}$ and $Gd_2O_2S:Er^{3+}_{(1\%)},Yb^{3+}_{(10\%)}$ materials prepared using Ln_2O_3 and $Ln(OH)CO_3$ as Ln source and were recorded with an Ekspla N342B OPO laser with a repetition rate of 10 Hz, a Triax 550 emission monochromator, and a Hamamatsu R928 PMT detector. For the Er^{3+} self-excitation lifetimes, the UC materials were excited at 520 and 661 nm while the emission was monitored at 554 and 670 nm for the green $^4S_{3/2}\rightarrow{}^4I_{15/2}$ and the red $^4F_{9/2}\rightarrow{}^4I_{15/2}$ emissions, respectively. For UC lifetimes, the materials were excited at 980 nm and the emission was collected also at 554 and 670 nm for the green and red emissions.

3. Results and discussion

3.1. MASS synthesis, phase purity and morphology of Gd_2O_2S-based UC materials

XRD patterns for the $Gd_2O_2S:Er^{3+}$ and $Gd_2O_2S:Er^{3+},Yb^{3+}$ UC materials prepared by the microwave-assisted solid-state (MASS) synthesis (Fig. 1) indicate that all materials were successfully produced in the Gd_2O_2S trigonal crystal structure (space group P$\overline{3}$m1, nº 164). This structural feature confirms that the two-step MASS synthesis of 25 min each step is suitable for preparing these materials.

The microwave-assisted particle formation mechanism of Gd_2O_2S was explored in a previous work [17]. In essence, the Gd_2O_3 + S + Na_2CO_3 precursor mixture is rapidly heated under microwave radiation with the activated carbon acting as the microwave susceptor. In this way, a transformation from Gd_2O_3 to Gd_2O_2S structure makes this the major crystal phase in less than 4 min of synthesis. The reaction involves sulfur atoms going through oxidation/reduction processes to be converted to S^{2-} ions and finally react with the Gd_2O_3 to form the Gd_2O_2S product. In this work, Er_2O_3 and Yb_2O_3 were also added in the precursor mixture to produce the $Gd_2O_2S:Er^{3+}$ and $Gd_2O_2S:Er^{3+},Yb^{3+}$ UC materials. Due to the smaller ionic radii of Er^{3+} (0.890 Å) and Yb^{3+} (0.868 Å) compared to Gd^{3+} (0.938 Å) and thus their harder-acid character [22], breaking Er–O and especially Yb–O bonds requires more energy than breaking Gd–O bonds [23]. This chemical feature increases the probability of Ln_2O_3 impurity phases in the final UC materials. Such impurities were not detected in the single-doped $Gd_2O_2S:Er^{3+}$ materials, but

small intensity diffraction peaks related to the c-Yb_2O_3 structure could be observed in the co-doped $Gd_2O_2S:Er^{3+},Yb^{3+}$ (Fig. 1a).

Although the Yb_2O_3 impurity is just a tiny fraction within the $Gd_2O_2S:Er^{3+},Yb^{3+}$ crystals, its presence confirms the lower reactivity of Yb_2O_3 which also affects the concentration and distribution of Yb^{3+} ions in the final product. Therefore, more reactive lanthanide hydroxycarbonates – $Ln(OH)CO_3$ (Ln^{3+}: Gd, Er, and Yb) were also investigated as lanthanide sources for the MASS synthesis, targeting pure phase Gd_2O_2S-based materials with a more homogeneous Yb^{3+} and Er^{3+} distribution. One can notice from the XRD patterns of the $Gd_2O_2S:Er^{3+}(,Yb^{3+})$ prepared using $Ln(OH)CO_3$ as precursors (Fig. 1b) that these materials do not show Er- or Yb_2O_3 impurities at any given dopant concentration. Some low intensity peaks can be observed in the $Gd_2O_2S:Er^{3+}_{(10\%)},Yb^{3+}_{(10\%)}$ material, but they were assigned to Al-related crystalline phases, probably originated from the alumina crucible. Clearly, the lanthanide hydroxycarbonates are better lanthanide precursors to prepare phase-pure oxysulfide materials with the MASS synthesis, as its thermal decomposition happens at considerably lower temperatures (500–700 °C) [20], facilitating the reaction with sulfide ions during the microwave synthesis. The use of $Ln(OH)CO_3$ precursor is also expected to enhance UC efficiency by increasing ion mobility and thus dopant homogeneity through the materials crystals lattice, as discussed below.

SEM images of the $Gd_2O_2S:Er^{3+}_{(10\%)}$ and $Gd_2O_2S:Er^{3+}_{(1\%)},Yb^{3+}_{(10\%)}$ materials were taken to investigate possible morphological differences between the materials prepared with different Ln sources – Ln_2O_3 or $Ln(OH)CO_3$ (Fig. 2). Distinct Ln sources had minor influences on the formed microcrystals, which range in size from 1 to 10 μm, exhibiting hexagonal-like shapes owing to the trigonal crystal structure of Gd_2O_2S. The materials prepared using $Ln(OH)CO_3$ showed a slightly more homogeneous particle size distribution compared to the ones produced using Ln_2O_3. Moreover, particle size and morphology seem independent of Er^{3+} and Yb^{3+} dopants and their concentrations. Similar results were obtained in a previous work [18] from $Gd_2O_2S:Tb^{3+}$ scintillator materials also prepared by the MASS synthesis. There, smaller crystal sizes of around 500 nm were synthesized by a shorter microwave synthesis time, *i.e.* 10 min instead of two heat treatments of 25 min each. By linking previous and recent results, the microwave synthesis time can be then defined as the predominant parameter rather than the used Ln sources to affect particle size and morphology. Nonetheless, longer microwave synthesis times, *e.g.* 2 × 25 min yield materials with higher degree of crystallinity and phase purity, and thus are better for improved optical properties [18].

Lastly, it its worth stating that $Gd_2O_2S:Er^{3+}$ and $Gd_2O_2S:Er^{3+},Yb^{3+}$ UC materials were prepared with high crystal purity in a rapid two-step synthesis of 50 min in total. Considering an oxysulfide preparation by conventional solid-state methods [15], the microwave-assisted solid-state synthesis lead to a remarkable decrease of 79% in processing time and 93% in energy consumption, making the MASS method suitable to be explored for diverse ceramic materials.

3.2. Optical properties of $Gd_2O_2S:Er^{3+}$ and $Gd_2O_2S:Er^{3+},Yb^{3+}$ UC materials

In this section, the optical properties of Gd_2O_2S-based upconversion materials prepared by the MASS synthesis were explored by evaluating the light emitted under IR-irradiation as a function of dopants and their concentrations, as well as the precursors used in the synthesis.

Under continuous 980 nm laser excitation, all synthesized materials exhibited visible range upconversion emission (Figure S2), arising from three main electronic transitions of Er^{3+} ion: $^2H_{11/2}\rightarrow{}^4I_{15/2}$ (523, 528, 533 nm), $^4S_{3/2}\rightarrow{}^4I_{15/2}$ (548, 554 nm), and $^4F_{9/2}\rightarrow{}^4I_{15/2}$ (max. 670 nm) (Fig. 3). For the Er^{3+} singly doped Gd_2O_2S, the highest UC emission intensity was measured for the highest dopant
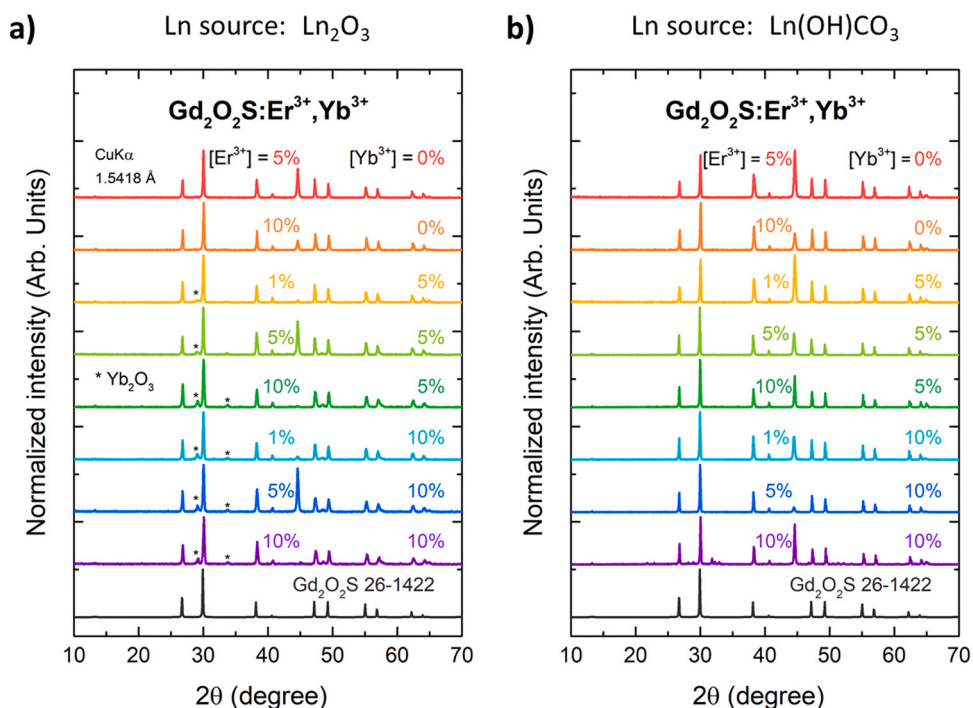
Fig. 1. Powder X-ray diffraction (XRD) patterns for the $Gd_2O_2S:Er^{3+}$ and $Gd_2O_2S:Er^{3+},Yb^{3+}$ upconversion (UC) materials prepared by the microwave-assisted solid-state (MASS) method ($2\theta = 45°$ peak corresponds to the Al substrate). Gd_2O_2S 26–1422 reference pattern was also displayed.

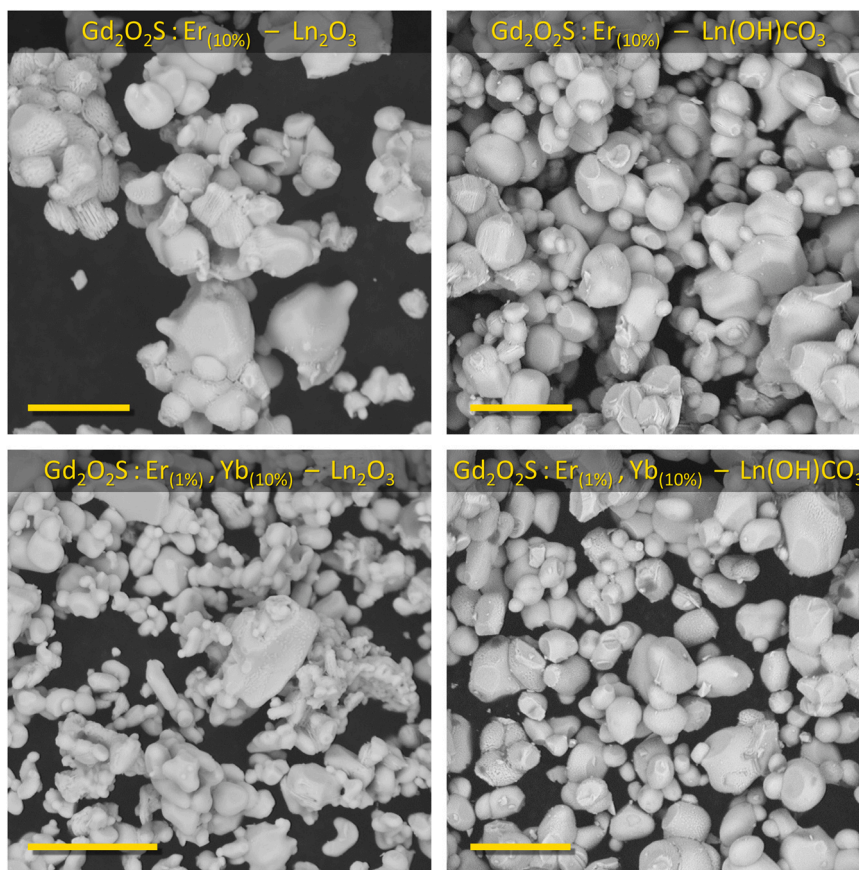**Fig. 2.** SEM images of the $Gd_2O_2S:Er^{3+}_{(10\%)}$ and $Gd_2O_2S:Er^{3+}_{(1\%)},Yb^{3+}_{(10\%)}$ materials, synthesized using lanthanide oxides (Ln_2O_3, left) and hydroxycarbonates ($Ln(OH)CO_3$, right) as Ln source for the MASS synthesis. Scale bar = 10 µm.
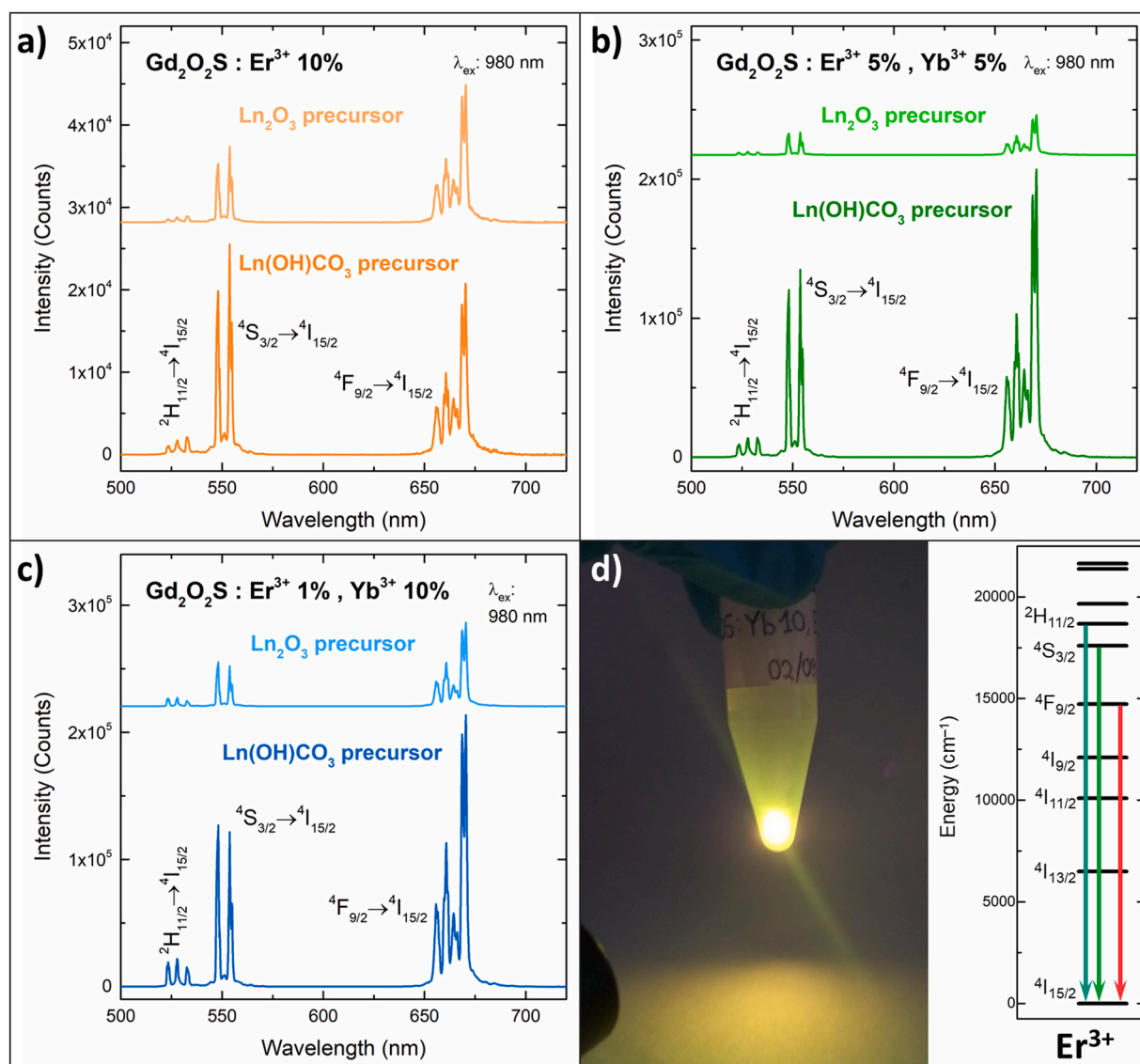
Fig. 3. Upconversion (UC) emission spectra of $Gd_2O_2S:Er^{3+}$ and $Gd_2O_2S:Er^{3+},Yb^{3+}$ materials synthesized by the MASS method using Ln_2O_3 and $Ln(OH)CO_3$ as the lanthanide source (Ln^{3+}: Gd, Er, and Yb): (a) $Gd_2O_2S:Er^{3+}_{(10\%)}$, (b) $Gd_2O_2S:Er^{3+}_{(5\%)},Yb^{3+}_{(5\%)}$, and (c) $Gd_2O_2S:Er^{3+}_{(1\%)},Yb^{3+}_{(10\%)}$ (the spectra of Ln_2O_3-based materials was shifted up in the Y-axis for better clarity). (d) UC emission of the $Ln(OH)CO_3$-based $Gd_2O_2S:Er^{3+}_{(1\%)},Yb^{3+}_{(10\%)}$ material under 980 nm laser excitation, together with the Er^{3+} energy level diagram showing the main UC emissions.

concentration, *i.e.* $Gd_2O_2S:Er^{3+}_{10\%}$ (Fig. 3a), while for the Er^{3+},Yb^{3+} co-doped samples, strongest UC emission were achieved by the $Gd_2O_2S:Er^{3+}_{(5\%)},Yb^{3+}_{(5\%)}$ (Fig. 3b) and $Gd_2O_2S:Er^{3+}_{(1\%)},Yb^{3+}_{(10\%)}$ materials (Fig. 3c,d).

Note that the recorded UC intensities can be directly compared between different samples – all measuring parameters, *e.g.* laser power and spot size in the sample, sample size and position, monochromator step size, and the integration time were optimized and fixed to allow the reliable detection of UC light intensities over many orders of magnitude from different materials. Results show that different Er^{3+} and Er^{3+},Yb^{3+} dopant concentrations yield substantial variations of overall UC intensities (Figure S2). Single-doped $Gd_2O_2S:Er^{3+}$ materials, especially the 10% Er^{3+} doped one (Fig. 3a), already show UC emission intense enough for imaging applications. When co-doped with Yb^{3+} ions, the $Gd_2O_2S:Er^{3+},Yb^{3+}$ materials achieve emission intensities up to one order of magnitude higher than their singly doped counterparts. This optical feature confirms the great importance of the Yb^{3+} sensitizer in increasing the absorption process and UC energy transfer within the Gd_2O_2S lattice due to the larger Yb^{3+} absorption cross-section.

Besides the Er^{3+},Yb^{3+} dopant concentrations, the Ln source compound used as precursors to the MASS synthesis also had a significant effect on the UC outcome. According to the UC emission spectra (Fig. 3a–c and Figure S2), changing the synthesis precursor from lanthanide oxides (Ln_2O_3) to lanthanide hydroxycarbonates ($Ln(OH)CO_3$) resulted in a drastic UC intensity increase for all Gd_2O_2S-based UC materials. This UC emission intensity increase was observed to be more pronounced for the Er^{3+},Yb^{3+} co-doped samples. We attribute this UC increase to the higher reactivity of the Ln-precursor, which helps in the formation of the Gd_2O_2S crystal lattice and increases doping homogeneity, thus enhancing energy migration processes.

Furthermore, the UC efficiency of MASS-prepared materials were directly compared with commercial samples (Leuchtstoffwerk Breitungen and Tailorlux), which have the same nominal concentrations of Er^{3+} and Yb^{3+} dopants (Fig. 4a and Figure S3). Based on an estimated 10% quantum efficiency for the Leuchtstoffwerk Breitungen $Gd_2O_2S:Er^{3+}_{10\%}$ material [12], the overall UC efficiencies of the various single-doped and co-doped UC materials were calculated from the integrated emission intensities in Figure S3. The highest UC
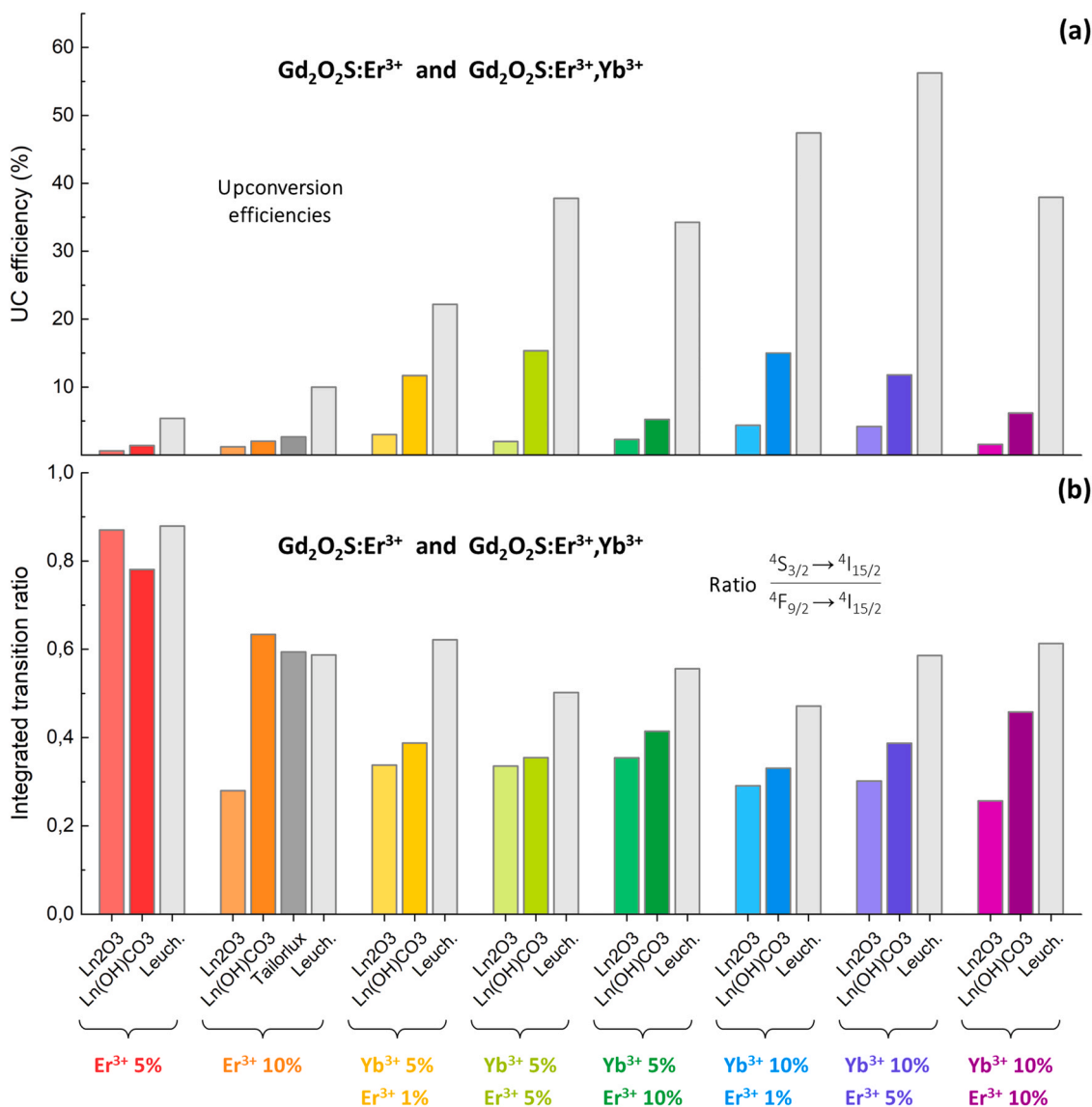
Fig. 4. (a) UC efficiencies calculated from all integrated emissions (Fig. S3), based on the previous estimate [12] of 10% efficiency for the single-doped $Gd_2O_2S:Er^{3+}_{(10\%)}$ commercial material from Leuchtstoffwerk Breitungen. (b) ($^4S_{3/2} \to {}^4I_{15/2}$) / ($^4F_{9/2} \to {}^4I_{15/2}$) transition ratios calculated for all $Gd_2O_2S:Er^{3+}(,Yb^{3+})$ UC materials as a function of dopant concentration.

efficiencies for the MASS-prepared materials are 2% for the $Gd_2O_2S:Er^{3+}_{(10\%)}$ (single-doped material) and around 15% for both $Gd_2O_2S:Er^{3+}_{(5\%)},Yb^{3+}_{(5\%)}$ and $Gd_2O_2S:Er^{3+}_{(1\%)},Yb^{3+}_{(10\%)}$, the most efficient co-doped materials (Table S1). In this way, the combination of dopant concentrations of $Er^{3+}_{(5\%)},Yb^{3+}_{(5\%)}$ and $Er^{3+}_{(1\%)},Yb^{3+}_{(10\%)}$ can be considered optimal to yield UC for the Gd_2O_2S host lattices synthesized by the MASS method. This is however not the case for the commercial materials, as the highest UC efficiency was calculated for the Leuchtstoffwerk Breitungen $Gd_2O_2S:Er^{3+}_{(5\%)},Yb^{3+}_{(10\%)}$ material (56%).

Essentially, these results show that the UC materials made with MASS method have a similar efficiency as the equivalent Tailorlux sample, while the efficiency of the Leuchtstoffwerk Breitungen UC materials are significantly higher (Table S1), which is consistent with an earlier comparison of the two types of commercial UC materials [12]. The higher efficiency of the materials from Leuchtstoffwerk Breitungen can be explained by the long experience of this company in making high quality $Gd_2O_2S:Pr^{3+}$ scintillator materials – in scintillators, the efficiency also strongly depends on the presence of impurities and defects that can capture free electrons and holes and thus reduce efficiency. Therefore, the higher UC efficiency of

Leuchtstoffwerk materials is due to the quality of these materials, more precisely the Er^{3+},Yb^{3+} doping homogeneity, In this way, even higher concentrations such as 5% of Er^{3+} and 10% of Yb^{3+} could be doped into the Gd_2O_2S host lattices without triggering losses mechanisms such as concentration quenching. The MASS synthesis, on the other hand, is a very short synthesis method, and thus doping homogeneity can be significantly lower compared to these commercial materials. Using $Ln(OH)CO_3$ as precursors aided in improving doping homogeneity as it can be seen from Table S1, where all $Ln(OH)CO_3$-based materials showed higher UC efficiencies compared to their Ln_2O_3-based counterparts. Nevertheless, it is worth stating that further optimization of the MASS method may lead to higher UC efficiencies that are closer to those of the best commercial materials. It is encouraging that the MASS method was able to produce materials with comparable intensity in a rapid (50 min) synthesis without any further treatment on the samples, which represents a promising ratio between photonic quality and time/cost of production.

In addition to the discussion on the UC efficiencies, the ratio between the integrated area of the green emission band ($^4S_{3/2} \to {}^4I_{15/2}$)

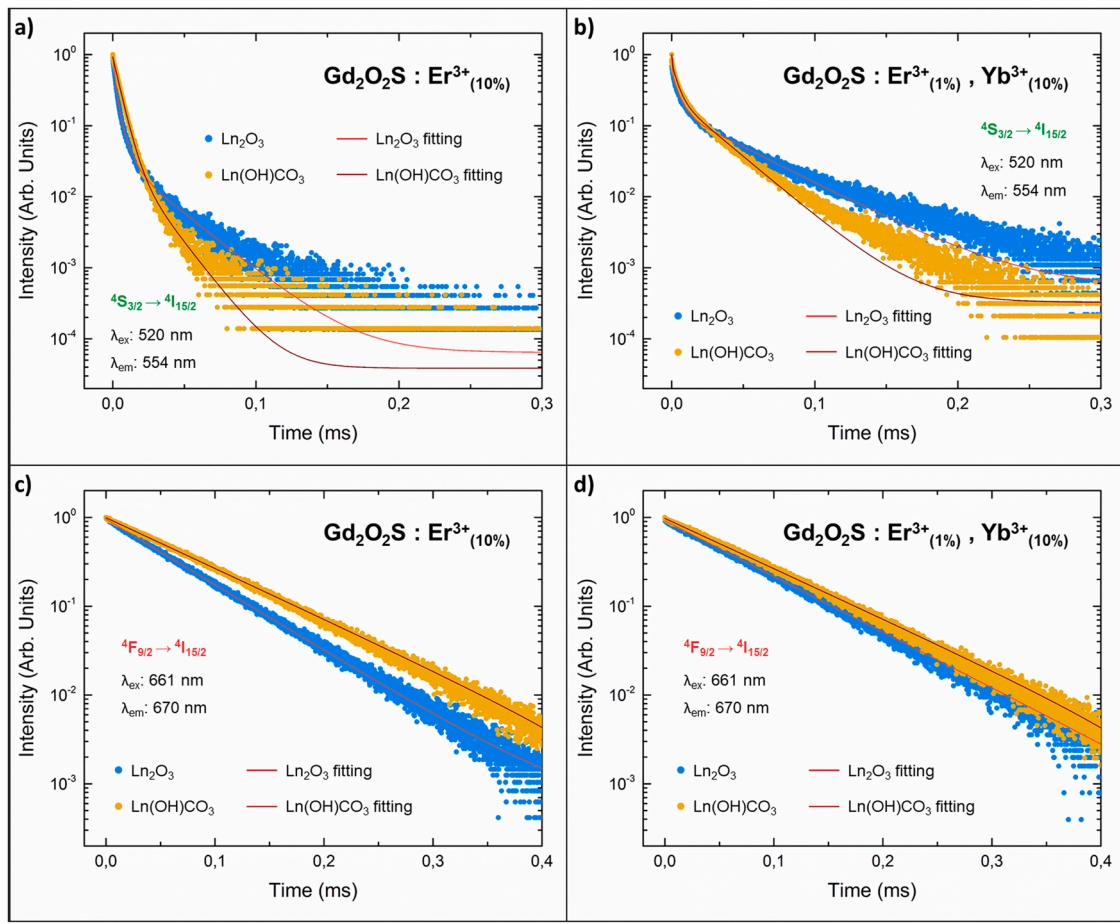**Fig. 5.** Luminescence decay curves of the $Gd_2O_2S:Er^{3+}_{(10\%)}$ and $Gd_2O_2S:Er^{3+}_{(1\%)},Yb^{3+}_{(10\%)}$ materials prepared using Ln_2O_3 and $Ln(OH)CO_3$ as the lanthanide source (Ln^{3+}: Gd, Er, and Yb). Monitoring the green $^4S_{3/2}\rightarrow{}^4I_{15/2}$ emission for the (a) $Gd_2O_2S:Er^{3+}_{(10\%)}$ and (b) $Gd_2O_2S:Er^{3+}_{(1\%)},Yb^{3+}_{(10\%)}$, and the red $^4F_{9/2}\rightarrow{}^4I_{15/2}$ emission for the (c) $Gd_2O_2S:Er^{3+}_{(10\%)}$ and (d) $Gd_2O_2S:Er^{3+}_{(1\%)},Yb^{3+}_{(10\%)}$.

and the red emission band ($^4F_{9/2}\rightarrow{}^4I_{15/2}$) was calculated for the MASS-prepared $Gd_2O_2S:Er^{3+}(,Yb^{3+})$ UC materials, as well as for the commercial samples (Fig. 4b). This ratio can be interpreted as an empirical parameter for the UC quenching from the green emitting $^4S_{3/2}$ to the red emitting $^4F_{9/2}$ level that depends on the Er^{3+},Yb^{3+} dopant concentration and distribution in the Gd_2O_2S host lattice. It is worth noting that especially the $^4S_{3/2}\rightarrow{}^4I_{15/2}$ emission can be quenched by cross-relaxation, thus higher Er^{3+} concentrations lead to a decrease in the ratio. For the same nominal concentrations, less homogeneous dopant distributions are expected to give lower ratios, as the $^4S_{3/2}$ emission will be more strongly quenched in Er-rich regions.

The results displayed in Fig. 4b show that the calculated ratio value is less than one for all measured samples, implying that the $^4F_{9/2}\rightarrow{}^4I_{15/2}$ transition has a higher integrated intensity for the Er^{3+},Yb^{3+} concentration ranges that are studied here. The highest ratios were found for singly doped $Gd_2O_2S:Er^{3+}$ materials. UC materials prepared using $Ln(OH)CO_3$ as Ln source precursor exhibited higher calculated ratios compared to its Ln_2O_3 counterparts. This suggests a reduced quenching from $^4S_{3/2}$ levels in the former materials, indicating that the use of $Ln(OH)CO_3$ precursors improves dopant ion homogeneity throughout the Gd_2O_2S crystal lattice. The positive effect of the hydroxycarbonate precursor on ion distribution and subsequently green/red ratio is corroborated by the relatively higher green/red ratios observed for the commercial samples. Such materials were synthesized by conventional solid-state methods, in which the long hours of heating at high temperatures (> 1000 °C) have significantly improved ion mobility and helped to achieve an even more homogeneous doping of Er^{3+} and Yb^{3+} ions.

Luminescence decay curves for UC materials are important to understand the dynamics of the excited states as a function of dopant concentration and its distribution within the crystal lattice [24,25]. Fig. 5 shows the self-excitation luminescence decay curves for the Er^{3+} $^4S_{3/2}\rightarrow{}^4I_{15/2}$ (5a,b) and $^4F_{9/2}\rightarrow{}^4I_{15/2}$ (5c,d) transitions in $Gd_2O_2S:Er^{3+}_{(10\%)}$ and $Gd_2O_2S:Er^{3+}_{(1\%)},Yb^{3+}_{(10\%)}$ materials synthesized using Ln_2O_3 and $Ln(OH)CO_3$ as the lanthanide source. The $^4S_{3/2}\rightarrow{}^4I_{15/2}$ emission decay show a multiexponential behavior due to the complex cross-relaxation and energy migration processes, and therefore were fitted as triexponential curves (except for the $Gd_2O_2S:Er^{3+}_{(10\%)}$ material prepared using $Ln(OH)CO_3$, which was fitted as a biexponential). From the calculated lifetimes (Table 2) one can see that

Table 2

Lifetime values (μs) of the Er^{3+} $^4S_{3/2}\rightarrow{}^4I_{15/2}$ and $^4F_{9/2}\rightarrow{}^4I_{15/2}$ transitions calculated for the $Gd_2O_2S:Er^{3+}_{(10\%)}$ and $Gd_2O_2S:Er^{3+}_{(1\%)},Yb^{3+}_{(10\%)}$ materials synthesized using Ln_2O_3 and $Ln(OH)CO_3$ as precursors (Ln^{3+}: Gd, Er, Yb). For the green $^4S_{3/2}\rightarrow{}^4I_{15/2}$ emission, lifetime values were obtained from fitting the data of Fig. 5a,b as triexponential decay curves (except for the $Ln(OH)CO_3$–based $Gd_2O_2S:Er^{3+}_{(10\%)}$ material, which was fitted as a biexponential). For the red $^4F_{9/2}\rightarrow{}^4I_{15/2}$ emission, lifetime values were obtained from fitting the data of Fig. 5c,d as monoexponential decay curves.

		$Gd_2O_2S:Er^{3+}_{(10\%)}$		$Gd_2O_2S:Er^{3+}_{(1\%)},Yb^{3+}_{(10\%)}$	
		Ln_2O_3 precursor	$Ln(OH)CO_3$ precursor	Ln_2O_3 precursor	$Ln(OH)CO_3$ precursor
$^4S_{3/2}$	τ_1	1.7 ± 0.0	4.8 ± 0.0	0.3 ± 0.0	0.1 ± 0.0
	τ_2	5.0 ± 0.1	–	4.7 ± 0.0	4.0 ± 0.0
	τ_3	26.9 ± 0.3	16.6 ± 0.3	42.6 ± 0.1	25.7 ± 0.1
$^4F_{9/2}$	τ_1	58.8 ± 0.0	76.1 ± 0.0	69.4 ± 0.0	76.9 ± 0.0

both Ln_2O_3-based UC materials have a faster initial component and a relatively slower long component. Although a similar behavior is observed for the $Ln(OH)CO_3$-based materials, the lifetime value discrepancy between the slower and the faster decay components is bigger for the former. This is an indicative for inhomogeneous doping, *i.e.* there are regions within the crystal with high dopant concentrations, which increases the probability of energy transfer processes (fast decay component), and regions where Er^{3+} has hardly any neighbors (long decay component). For the materials prepared using $Ln(OH)CO_3$ as precursors, the more homogeneous dopant dispersion causes the overall lifetime to be slightly shorter.

The decay curves for the $^4F_{9/2} \rightarrow ^4I_{15/2}$ transition showed a monoexponential decay profile (Fig. 5c,d). The fitted decay lifetime values (Table 2) show slightly longer lifetimes for the $Ln(OH)CO_3$-based materials compared to the Ln_2O_3-based ones. Although these results seem conflicting, it is worth noting that cross-relaxation processes between Er^{3+} neighbors, as well as energy transfer from the $^4S_{3/2}$ level to a neighboring Yb^{3+} ion (accompanied by phonon emission), can depopulate the $^4S_{3/2}$ level more strongly than for the $^4F_{9/2}$ level. This is corroborated by the different behaviors of the $^4S_{3/2} \rightarrow ^4I_{15/2}$ (multiexponential) and $^4F_{9/2} \rightarrow ^4I_{15/2}$ (monoexponential) transitions. This optical features explains the faster initial decay and shorter lifetime for the $^4S_{3/2}$ emission compared to the $^4F_{9/2}$ (Table 2) [16]. Furthermore, similar results were observed on the UC lifetime decay curves for the $Gd_2O_2S:Er^{3+}_{(1\%)},Yb^{3+}_{(10\%)}$ materials (Figure S4). These decay curves were fitted as monoexponentials after excluding the first data points corresponding to the rise time. The resultant lifetime values were compiled in Table S2, where longer lifetimes can be observed for the $Gd_2O_2S:Er^{3+}_{(1\%)},Yb^{3+}_{(10\%)}$ material prepared using $Ln(OH)CO_3$ compared to the one prepared using Ln_2O_3. All together, these results confirm the better suitability of hydroxycarbonates as precursors for high quality optical materials and better dopant ion distribution by using the microwave synthesis.

4. Conclusion

In this work, Er^{3+}-doped and Er^{3+},Yb^{3+}-co-doped Gd_2O_2S were prepared by the microwave-assisted solid-state (MASS) synthesis, producing efficient upconversion (UC) materials. The syntheses were performed in a domestic 1 kWh microwave oven in 2 steps of 25 min each, using two different lanthanide precursors – Ln_2O_3 and $Ln(OH)CO_3$, where Ln^{3+}: Gd, Er, Yb. In addition, materials were prepared with several Er^{3+},Yb^{3+} dopant concentrations to investigate the optimal concentration for the highest UC intensity and compare with commercial samples. Co-doped $Gd_2O_2S:Er^{3+},Yb^{3+}$ materials were shown to have superior UC performance over the single-doped $Gd_2O_2S:Er^{3+}$ ones – 2% of UC efficiency was estimated for the $Gd_2O_2S:Er^{3+}_{(10\%)}$ material, while the most efficient co-doped materials, *i.e.* $Gd_2O_2S:Er^{3+}_{(5\%)},Yb^{3+}_{(5\%)}$ and $Gd_2O_2S:Er^{3+}_{(1\%)},Yb^{3+}_{(10\%)}$ showed UC efficiencies around 15%. Moreover, such efficiencies were 3–8 times higher when using $Ln(OH)CO_3$ instead of Ln_2O_3 as starting materials. Lifetime decay measurements explained this improvement by a more homogeneous distribution of dopant ions and possibly a higher crystallinity (less defects) when using the more reactive hydroxycarbonate precursor. The highest UC emission intensity among the MASS-prepared materials where observed to be only 2–3 times less bright than the best commercial UC materials with same nominal Er^{3+},Yb^{3+} dopant concentrations. Therefore, the MASS synthesis was demonstrated to be a rapid and energy-saving method to prepare high crystalline and optical quality UC materials, being a cost-effective and environmentally friendly method suitable for large-scale production.

Data Availability

No data was used for the research described in the article.

Declaration of Competing Interest

The authors declare that they have no known competing financial interests or personal relationships that could have appeared to influence the work reported in this paper.

Author contributions

I.P.M., C.S.S.P., and A.M. conceived the scientific idea. I.P.M. synthesized the UC materials by the MASS method, and I.P.M., J.W., and A.V.B. performed the characterization and upconversion experiments. [16] V.R., H.F.B., and A.M. supervised the work, contributing to the interpretation and discussion of the results. All authors have given approval to the final version of the manuscript.

Appendix A. Supporting information

Supplementary data associated with this article can be found in the online version at doi:10.1016/j.jallcom.2023.169083.

References

[1] F. Auzel, History of upconversion discovery and its evolution, J. Lumin. 223 (2020) 116900.
[2] X. Zhu, J. Zhang, J. Liu, Y. Zhang, Recent progress of rare-earth doped upconversion nanoparticles: synthesis, optimization, and applications, Adv. Sci. 6 (2019) 1901358.
[3] F. Auzel, Upconversion and anti-stokes processes with f and d ions in solids, Chem. Rev. 104 (2004) 139–173.
[4] I. Hyppänen, J. Hölsä, J. Kankare, M. Lastusaari, L. Pihlgren, Up-conversion luminescence properties of $Y_2O_2S:Yb^{3+},Er^{3+}$ nanophosphors, Opt. Mater. 31 (2009) 1787–1790.
[5] A. Shalav, B.S. Richards, T. Trupke, K.W. Krämer, H.U. Güdel, Application of $NaYF_4:Er^{3+}$ up-converting phosphors for enhanced near-infrared silicon solar cell response, Appl. Phys. Lett. 86 (2005) 1–4.
[6] V. Kataria, D.S. Mehta, Impact of firing temperature on multi-wavelength selective stokes and anti-stokes luminescent behavior by $Gd_2O_2S:Er,Yb$ phosphor and its application in solar energy harvesting, J. Phys. D. Appl. Phys. 51 (2018) 145501.
[7] S. Fischer, A. Ivaturi, P. Jakob, K.W. Krämer, R. Martin-Rodriguez, A. Meijerink, B. Richards, J.C. Goldschmidt, Upconversion solar cell measurements under real sunlight, Opt. Mater. 84 (2018) 389–395.
[8] D.K. Chatterjee, A.J. Rufaihah, Y. Zhang, Upconversion fluorescence imaging of cells and small animals using lanthanide doped nanocrystals, Biomaterials 29 (2008) 937–943.
[9] N.M. Idris, M.K. Gnanasammandhan, J. Zhang, P.C. Ho, R. Mahendran, Y. Zhang, In vivo photodynamic therapy using upconversion nanoparticles as remote-controlled nanotransducers, Nat. Med. 18 (2012) 1580–1585.
[10] J.C. Boyer, F.C.J.M. van Veggel, Absolute quantum yield measurements of colloidal $NaYF_4:Er^{3+},Yb^{3+}$ upconverting nanoparticles, Nanoscale 2 (2010) 1417–1419.
[11] X. Luo, W. Cao, Blue, green, red upconversion luminescence and optical characteristics of rare earth doped rare earth oxide and oxysulfide, Sci. China Ser. B 50 (2007) 505–513.
[12] R. Martín-Rodríguez, S. Fischer, A. Ivaturi, B. Froehlich, K.W. Krämer, J.C. Goldschmidt, B.S. Richards, A. Meijerink, Highly efficient IR to NIR upconversion in $Gd_2O_2S:Er^{3+}$ for photovoltaic applications, Chem. Mater. 25 (2013) 1912–1921.
[13] J. Hölsä, T. Laamanen, M. Lastusaari, M. Malkamäki, J. Niittykoski, E. Zych, Effect of Mg^{2+} and Ti^{IV} doping on the luminescence of $Y_2O_2S:Eu^{3+}$, Opt. Mater. 31 (2009) 1791–1793.
[14] C.L. Lo, J.G. Duh, B.S. Chiou, C.C. Peng, L. Ozawa, Synthesis of Eu^{3+}-activated yttrium oxysulfide red phosphor by flux fusion method, Mater. Chem. Phys. 71 (2001) 179–189.
[15] Y. Ding, Z. Zhang, L. Wang, Q. Zhang, S. Pan, The role of sodium compound fluxes used to synthesize $Gd_2O_2S:Tb3+$ by sulfide fusion method, J. Mater. Sci. Mater. El. 28 (2017) 2723–2730.
[16] F.T. Rabouw, P.T. Prins, P. Villanueva-Delgado, M. Castelijns, R.G. Geitenbeek, A. Meijerink, Quenching Pathways in $NaYF_4:Er^{3+},Yb^{3+}$ upconversion Nanocrystals, ACS Nano 12 (2018) 4812–4823.

[17] J.M. Carvalho, C.C.S. Pedroso, I.P. Machado, J. Hölsä, L.C.V. Rodrigues, P. Głuchowski, M. Lastusaari, H.F. Brito, Persistent luminescence warm-light LEDs based on Ti-doped RE_2O_2S materials prepared by rapid and energy-saving microwave-assisted synthesis, J. Mater. Chem. C. 6 (2018) 8897–8905.

[18] I.P. Machado, V.C. Teixeira, C.C.S. Pedroso, H.F. Brito, L.C.V. Rodrigues, X-ray scintillator Gd_2O_2S:Tb3+ materials obtained by a rapid and cost-effective microwave-assisted solid-state synthesis, J. Alloy. Compd. 777 (2019) 638–645.

[19] I.P. Machado, C.C.S. Pedroso, J.M. Carvalho, V.C. Teixeira, L.C.V. Rodrigues, H.F. Brito, A new path to design near-infrared persistent luminescence materials using Yb^{3+}-doped rare earth oxysulfides, Scr. Mater. 164 (2019) 57–61.

[20] L.M. D'Assunção, M. Ionashiro, I. Giolito, Thermal decomposition of the hydrated basic carbonates of lanthanides and yttrium in CO_2 atmosphere, Thermochim. Acta 219 (1993) 225–233.

[21] J.M. Luiz, J.R. Matos, I. Giolito, M. Ionashiro, Thermal behaviour of the basic carbonates of lanthanum-europium, Thermochim. Acta 254 (1995) 209–218.

[22] R.G. Pearson, Hard and soft acids and bases, J. Am. Chem. Soc. 85 (1963) 3533–3539.

[23] G.Y. Adachi, N. Imanaka, The binary rare earth oxides, Chem. Rev. 98 (1998) 1479–1514.

[24] R. Martín-Rodríguez, F.T. Rabouw, M. Trevisani, M. Bettinelli, A. Meijerink, Upconversion dynamics in Er^{3+}-doped Gd_2O_2S: influence of excitation power, Er^{3+} concentration, and defects, Adv. Opt. Mater. 3 (2015) 558–567.

[25] F. Wang, R. Deng, J. Wang, Q. Wang, Y. Han, H. Zhu, X. Chen, X. Liu, Tuning upconversion through energy migration in core-shell nanoparticles, Nat. Mater. 10 (2011) 968–973.